**Supplemental Figures**

**Figure S1**

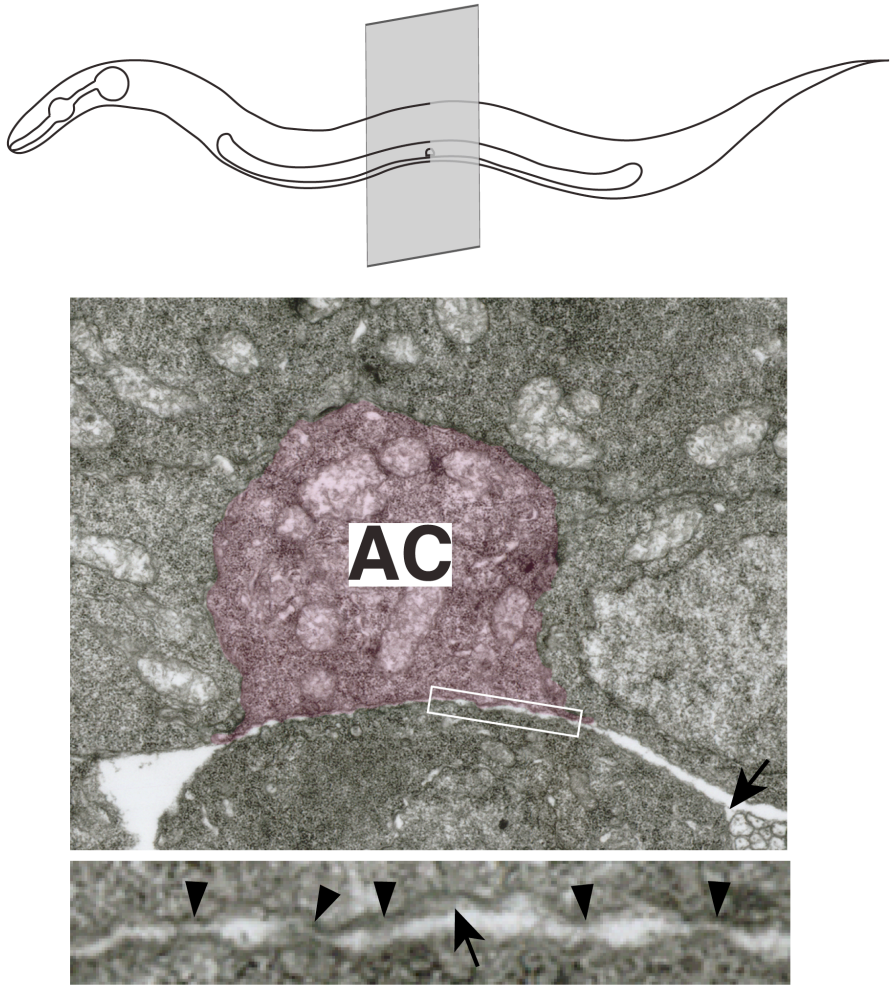


**Figure S1, related to Figure 1. Transverse TEM view of AC-BM attachment.** An archival series of thin sections identified the AC prior to invasion from the transverse perspective (transverse section of worm schematically illustrated). This series of thin sections was originally collected by Doug Kershaw in the laboratory of Sydney Brenner at the MRC and is now curated by the Hall lab. The AC is pseudocolored magenta. A region corresponding to the boxed area (shown below) reveals electron dense structures (arrowheads) connecting the gonadal and ventral BMs (arrows).

## Figure S2

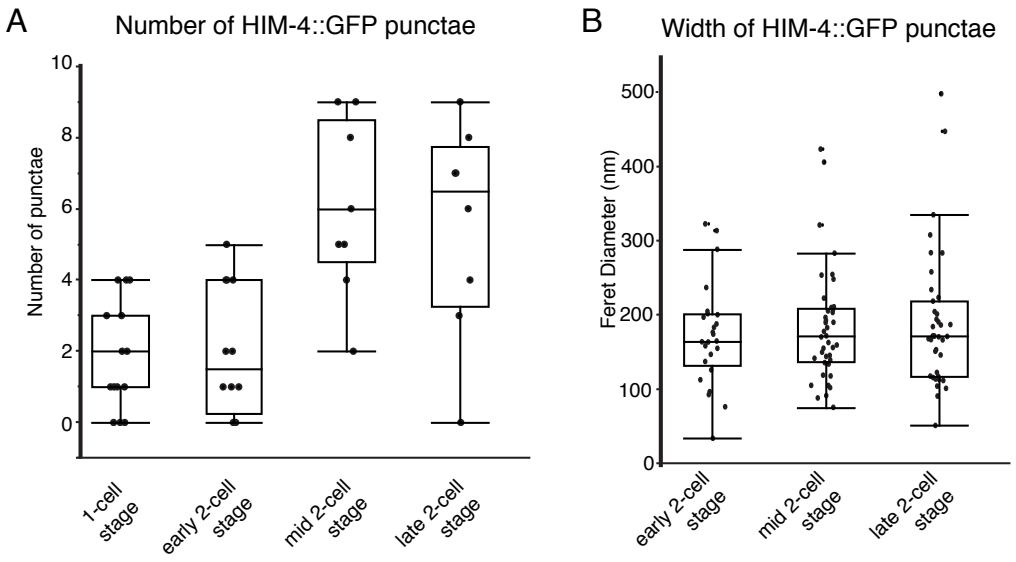


**Figure S2, related to Figure 2. Number and size of hemicentin punctae under the AC.** Graphs quantify hemicentin punctae number (A) and width (B) prior to and during AC invasion (n=104 structures in 23 worms). Boxes show the interquartile range and whiskers represent 1.5x interquartile range.

## Figure S3

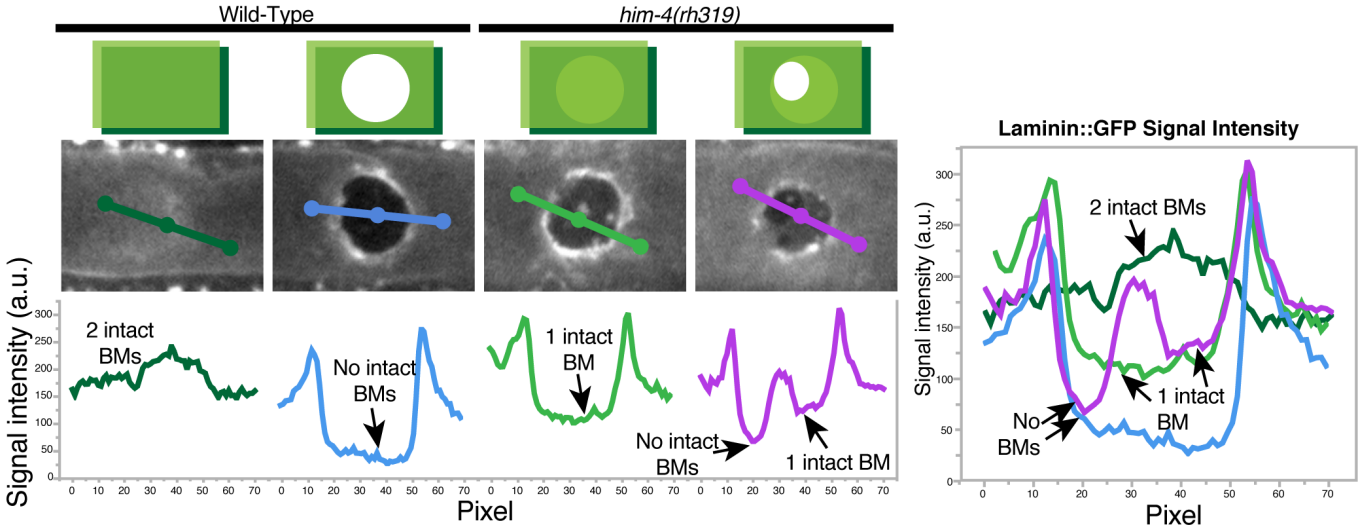


**Figure S3, related to Figure 3. Analysis of fluorescence intensity along no BM breach, single BM breach and double BM breaches.** Schematics (top panel) of sum fluorescence projections (middle) show a worm with no BM breach (left), both BMs breached (center left and right), one BM breached (center right). The intensity of sum fluorescence projections was analyzed along the line depicted and graphed (bottom). The graphs are overlayed (right) to highlight the changes in fluorescence intensity when zero, one or two BMs are present.

**Figure S4**

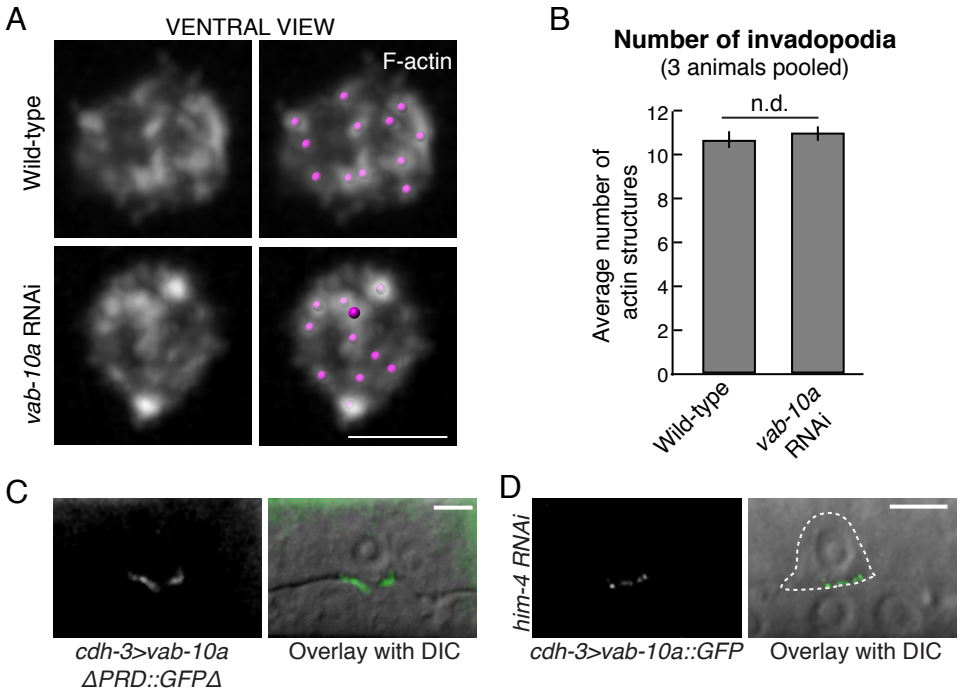


**Figure S4, related to Figure 4. The role of VAB-10A in BM-BM attachment.** (A) A ventral view of the AC shows F-actin rich invadopodia along the AC-BM interface (AC-specific F-actin probe, *cdh-3*>mCherry::moeABD) in a wild-type and an animal treated with *vab-10a* RNAi. (B) Graph depicts the average number of actin structures in wild-type and animals treated with *vab-10a* RNAi (10.6±0.4 structures present in wild-type, 10.9±0.3 structures present in *him-4(rh319)*, n=93 time points in 3 animals for each treatment; p=0.3, Wilcoxon Rank-Sum test, error bars denote SEM). (C) Lateral view of an AC expressing VAB-10AΔPRD::GFP shows that VAB-10A lacking all plectin repeat domains is enriched at the invasive membrane (n=9/9 worms expressing VAB-10AΔPRD::GFP in the AC). (D) Reduction of hemicentin (*him-4(RNAi)*) did not change the localization of VAB-10A::GFP (n=12/13 animals; GFP alone, left; overlaid with DIC, right). AC is outlined by dashed line. Scale bars, 5µm.

## Figure S5

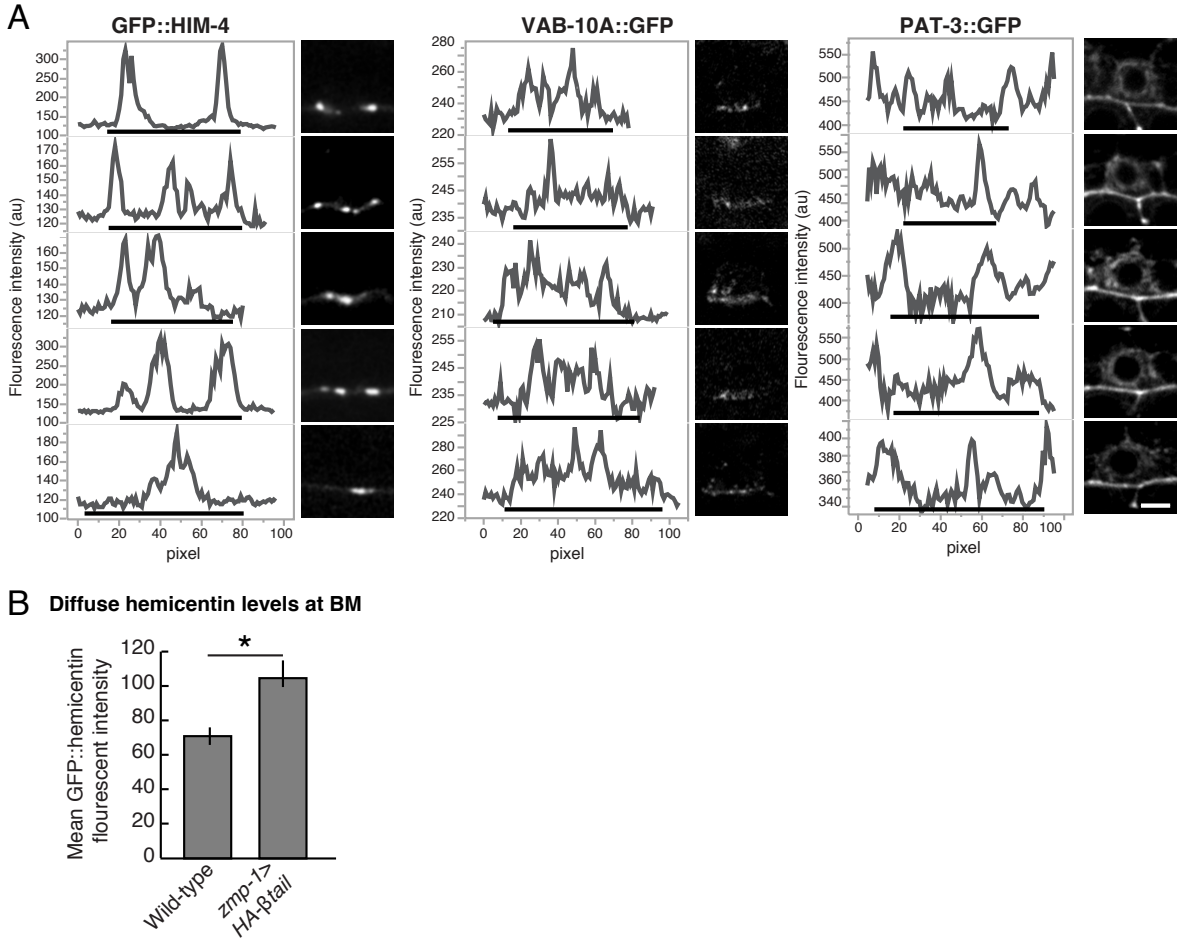


**Figure S5, related to Figure 5. Relationship between integrin, hemicentin and VAB-10A localization.** (A) Linescans (left) taken along the AC-BM interface in representative images (right) show fluorescence intensity of components of the BM-BM adhesion system. The region of the linescan that corresponds with the AC footprint is underlined. Hemicentin (GFP::hemicentin, left) accumulates into discrete punctae that appear as steep peaks in the linescans. VAB-10A (*cdh-3*>VAB-10A::GFP, center) and integrin (PAT-3::GFP, right) are distributed more evenly along the ACs invasive cell membrane. The graphs have been scaled to emphasize the distribution of the signal, not the variation in fluorescence intensity between animals. (B) The average fluorescence intensity of

diffuse hemicentin in the BMs under the AC was increased after loss of integrin function in the AC (ACs expressing *zmp-1*>HA-βtail; n=18 wild-type animals and 11 animals expressing HA–β-tail, $p<0.05$, Student's *t*-test, error bars show SEM). Scale bars, 5μm.

**Table S1, related to Table 1.**
***C. elegans* gene homology.**

| ***C. elegans* gene** | **Homology** |
|---|---|
| *him-4* | Hemicentin |
| *vab-10a* | Plakin; related to plectin |
| *vab-10b* | Plakin; related to BPAG1 and MCAF |
| *git-1* | Git1 homolog, G-protein coupled receptor kinase interactor |
| *let-805* | Transmembrane adhesion receptor |
| *mua-3* | Matrilin-like; transmembrane adhesion receptor |
| *mup-4* | Matrilin-like; transmembrane adhesion receptor |
| *pak-1* | Pak homolog |
| *pix-1* | Pix homolog |
| *eps-8* | Eps8 homolog; actin capping protein |
| *vab-19* | Kank homolog; ankyrin-repeat containing protein |
| *dgn-1* | dystroglycan |
| *dgn-2* | dystroglycan |
| *dgn-3* | all dystroglycan orthologs |
| *gpn-1* | glypican |
| *lon-2* | glypican |
| *ina-1* | α integrin subunit |
| *pat-3* | β integrin subunit |
| *pat-2* | α integrin subunit |
| *ptp-3* | receptor-like tyrosine phosphatase |
| *sdn-1* | syndecan |
| *ten-1* | teneruin |

**Table S2, related to Table 1.**
**Hemicentin deposition.**

| RNAi target | % with punctae | % with no punctae | n= |
|---|---|---|---|
| *git-1* | 71[a] | 29 | 24 |
| *let-805* | 82 | 18 | 28 |
| *mua-3* | 92 | 8 | 26 |
| *mup-4* | 85 | 15 | 26 |
| *pak-1* | 95 | 5 | 22 |
| *vab-10* | 93 | 7 | 14 |
| *eps-8* | 91 | 9 | 11 |
| *vab-19* | 87 | 13 | 15 |

[a] Punctae assembly was analyzed using *rhIs23(GFP::hemicentin)*

**Table S3, related to Table 1.**
**Screen of BM receptors and intermediate filaments.**

| Genotype/Treatment | % Block[a] | *n*= |
|---|---|---|
| **Screen of BM receptors** | | |
| *dgn-1(cg121)* | 0 | 50 |
| *dgn-2(ok209)*[b] | 0 | 27 |
| *dgn-1(cg121), dgn-2(ok209), dgn-3(tm1092)* | 0 | 21 |
| *gpn-1(ok377)*[b] | 0 | 13 |
| *lon-2(e678)*[b] | 0 | 13 |
| *ina-1(RNAi), rrf-3(pk1426)*[c] | 22 | 74 |
| *pat-3(RNAi), rrf-3(pk1426)*[c] | 58 | 82 |
| *pat-2(RNAi), rrf-3(pk1426)*[c] | 0 | 31 |
| *ptp-3(op147)*[b] | 0 | 10 |
| *sdn-1(ok449)*[b] | 0 | 13 |
| *ten-1(ok641)* | 0 | 38 |
| **Screen of intermediate filaments** | | |
| *L4440, qyIs101*[d] | 0 | 68 |
| *ifa-1(RNAi), qyIs101* | 0 | 30 |
| *ifa-2(RNAi), qyIs101* | 0 | 30 |
| *ifa-3(RNAi), qyIs101* | 0 | 13 |
| *ifa-4(RNAi), rrf-3(pk1426)* | 0 | 22 |
| *ifb-1(RNAi),qyIs101* | 2 | 54 |
| *ifb-2(RNAi), qyIs101* | 0 | 30 |
| *ifc-1(RNAi), qyIs101* | 0 | 31 |
| *ifc-2(RNAi), qyIs101* | 5 | 22 |
| *ifd-1(RNAi), qyIs101* | 3 | 30 |
| *ifd-2(RNAi), qyIs101* | 3 | 30 |
| *ife-1(RNAi), qyIs101* | 0 | 30 |

[a] ACs showing any degree of invasion were scored as invaded. In contrast, Table 1 shows partial AC invasion in addition to complete blocks. [b] Data from Ziel et al. 2009. [c] Data from Hagedorn et al. 2009. [d] *qyIs101* encodes FP-4 mito, which sensitizes the worms to perturbations in AC invasion by sequestering UNC-34 to the mitochondria.

**Supplemental Movie Legends**

**Movie S1, related to Figure 2. Hemicentin dynamics in wild-type animals.** A ventral view timelapse shows static hemicentin punctae (GFP::hemicentin, green) beneath the AC. This is in contrast to dynamic F-actin within the AC (*cdh-3*>mCherry::moeABD). A one hour timelapse is shown with frames acquired every 60 s. Scale bar, 5µm.

**Movie S2, related to Figure 2. Hemicentin punctae are pushed aside with the BM during AC invasion.** A ventral view timelapse shows hemicentin punctae (center, white; right, green) being pushed aside with the BM as the AC (*cdh-3*>mCherry::moeABD, left, white; right, magenta). A one hour timelapse is shown with frames acquired every 60 s. Scale bar, 5µm.

**Movie S3, related to Figure 3. Hemicentin mutants breach the ventral BM in a delayed manner.** Two ventral view timelapses shows a wild-type and hemicentin mutant animal breaching the ventral BM. Notably, the hemicentin worm is two hours older than the wild-type worm at the start of the timelapse. A 90 minute timelapse is shown with frames acquired every 120 s. Scale bar, 5µm.

## Supplemental Methods

### Targeted screen and RNA interference

A targeted screen of hemidesmosomes components was conducted by analyzing genes with the GO term 'hemidesmosome' (GO:0030056, 9/06/12) for defects in AC invasion. RNA interference (RNAi) was delivered by feeding worms E. coli expressing double-stranded RNA (dsRNA). Clones for RNAi targeting *mua-3* and *mup-4* were acquired from the Ahringer library and clones for *let-805*, *git-1*, *pak-1* and *eps-8* were acquired from the Vidal ORFeome library (Kamath and Ahringer, 2003; Rual et al., 2004). The RNAi clone targeting *vab-10a* was created by inserting the previously reported *vab-10a*-specific RNAi sequence (Bosher et al., 2003) positions 14630-15756 of ZK1151) into the L4440 RNAi expression vector. The RNAi clone targeting *vab-10b* was created by inserting positions 2018 and 3136 of ZK1151 into L4440. While this *vab-10b* RNAi sequence has been previously reported to produce phenotypes similar to *vab-10b(mc44)* when used in conjunction with a second dsRNA (positions 5807 of *Y47H9B* and 518 of *ZK1151*; (Bosher et al., 2003)), we found that feeding the RNAi targeting 2018-3136 of ZK1151 alone was sufficient to cause muscle attachment defects in the L4 larva, while feeding the second RNAi construct caused no noticeable defects by the time of AC invasion.

To bypass embryonic lethality, synchronized L1 stage larvae were plated RNAi. Plating L1 larva on RNAi targeting *vab-10a*, *mua-3* or *mup-4* caused larval arrest, thus synchronized L2 stage larvae were plated on RNAi 24 hours before AC invasion. The empty RNAi vector L4440 was used as a negative control. RNAi vectors were sequenced to verify correct insert.

**Construction of *vab-10a::GFP* fusions**

The endogenous *vab-10* locus was tagged with GFP using the recently described CRIPSR-Cas9 technique (Dickinson et al., 2013). Briefly, an sgRNA with the sequence 5'-gtatacatgacgctaagaa-3' targeted Cas9 to induce a double strand break near the final exon of *vab-10a*. The double stranded break was repaired from a construct containing 1.5-2 KB of 5' and 3' genomic regions, a GFP tag in place of the stop codon of the final *vab-10a* exon and *cbr-unc-119* following the endogenous 5' UTR. AC specific *vab-10a::GFP* was created by amplifying the following sections from cDNA and inserting them into pBsSK containing the *cdh-3*$^{mk62-63}$ promoter element (Kirouac and Sternberg, 2003): 1-1218 (Xba1-Xma1), 1219-8394 (Xma1-Mlu1), 8395-10308 (Mlu1-Kpn1). The stop codon was replaced with GFP. This construct was injected into *unc-119(ed4)* worms along with 50 ng/µl unc-119 rescue DNA, 50 ng/µl pBsSK and 50 ng/µl EcoR1 cut salmon sperm. *cdh-3>vab-10aΔPRD::GFP* was created by deleting *vab-10a* 4771-10308 from the *cdh-3>vab-10a::GFP* construct.